Journal of Adhesion Science and Technology

Publication details, including instructions for authors and subscription information:
http://www.tandfonline.com/loi/tast20

In Situ Observation of Thermal Marangoni Convection on the Surface of a Sessile Droplet by Infrared Thermal Imaging

Ziqian Wang [a] & Ya-Pu Zhao [a]

[a] State Key Laboratory of Nonlinear Mechanics (LNM), Institute of Mechanics, Chinese Academy of Sciences, Beijing, 100190, People's Republic of China

Version of record first published: 17 May 2012.

To cite this article: Ziqian Wang & Ya-Pu Zhao (2012): In Situ Observation of Thermal Marangoni Convection on the Surface of a Sessile Droplet by Infrared Thermal Imaging, Journal of Adhesion Science and Technology, 26:12-17, 2177-2188

To link to this article: http://dx.doi.org/10.1163/156856111X600523

VSP Journal of Adhesion Science and Technology 26 (2012) 2177–2188

Journal of ADHESION SCIENCE and TECHNOLOGY
brill.nl/jast

In Situ Observation of Thermal Marangoni Convection on the Surface of a Sessile Droplet by Infrared Thermal Imaging

Ziqian Wang and Ya-Pu Zhao *

State Key Laboratory of Nonlinear Mechanics (LNM), Institute of Mechanics, Chinese Academy of Sciences, Beijing 100190, People's Republic of China

Abstract

An *in situ* observation method to understand thermal Marangoni convection in sessile droplets is reported in this paper. Infrared (IR) thermal imaging is applied in the experiments to visualize the transient temperature distribution on the surface of the droplet. Additionally, micro particle image velocimetry (micro-PIV) system illustrates the fluid field inside the droplet. Two kinds of droplets are considered in this paper: sessile droplets heated with a hotplate and droplets heated by an electrode at the apex. Convection in both droplets is observed *in situ*, and the experimental results are in accord with the theory of fluid mechanics.

Keywords

Electrowetting, Marangoni convection, sessile droplet, infrared thermal imaging

Notations

k thermal coefficient

n empirical factor

R radius of the spherical cap

T temperature

T_c critical temperature in Kelvin

α thermal diffusivity

γ surface tension

γ_0 reference surface tension at $T = 0°C$

* To whom correspondence should be addressed. Tel.: (86-10) 8254-3932; Fax: (86-10) 8254-3977; e-mail: yzhao@imech.ac.cn

DOI:10.1163/156856111X600523

γ^* surface tension at $T = T_c$

$\Delta\gamma$ surface tension difference

ν kinematic viscosity

ρ density of the liquid

List of Abbreviations

AC alternating current

CCD charge-coupled device

DC direct current

EEC electro-elasto-capillarity

EWOD electrowetting on dielectric

IR infrared

ITO indium tin oxide

LOC lab-on-a-chip

Ma Marangoni number

PCR polymerase chain reaction

PDMS poly(dimethylsiloxane)

PIV particle image velocimetry

qPCR quantitative polymerase chain reaction

1. Introduction

Knowledge of the Marangoni convection behavior of individual sessile droplets is not only essential for the understanding of the internal heat and mass transfer in the droplets, but also important in the area of engineering [1–11], such as crystal growth and inkjet printing. In electro-elasto-capillarity (EEC) [2], involving controllable and reversible wrapping of droplet by a soft thin film, the process will be influenced by the convection induced by electric field and thermal field. With the development of lab-on-a-chip (LOC) devices, the droplets' behavior is attracting much interest of researchers, since nearly all LOC experiments are based on microscale fluid behaviors, such as micro droplets and liquid in micro channel. For micro quantitative polymerase chain reaction (micro qPCR) in micro pool [12], the thermal Marangoni convection behavior directly influences the temperature uniformity in the microscale pool, in which the capillary number is much smaller than 1 and the Bond Number is also small. Joule heat produced in microfabrication or

plasmon decay in a nanostructure will also be sufficient to induce Marangoni convection in droplet [13–16]. In the case of electrowetting on dielectric (EWOD), the thermal behavior and convection in droplets in both stable and instable situations are also of interest [17, 18].

Marangoni convection is associated with surface tension gradient [18], which results from temperature non-uniformity on the surface, concentration gradient or even by electric field. Theoretical analysis and numerical simulations of Marangoni convection in a sessile droplet were well developed in the past decades, however, papers concerning *in situ* observation of such convection are not often seen.

Temperature gradient induced Marangoni convection is observed *in situ* in the present study with the help of an infrared (IR) thermal imager (Fluke Ti-55). In order to continually visualize the temperature distribution on the surface of a millimeter scale droplet, Fluke 100 μm focus close-up lens was used. The IR thermal imager was fixed on a special tripod to avoid vibration and to improve photo quality. The application of IR camera is also seen in the work of Wen and coworkers [19, 20], where the camera was used to obtain the surface temperature distribution of micro-heater made of conductive poly(dimethylsiloxane) (PDMS) in static state.

Micro particle image velocimetry (micro-PIV) system is an effective method to quantitatively measure fluid fields in microscale, such as droplets or microchannels. In the work of Kang and coworkers, fluid field in the droplet in the case of AC voltage driven EWOD was observed by micro-PIV system [18]. In the present study, micro-PIV system was applied to visualize the fluid field inside the droplet heated by two different heating sources. In this study, transient temperature distribution field progressing in heated droplet was first observed by an IR thermal imager, which was of importance for obtaining detailed information on droplet convection and evaporation behavior. Two types of droplets were considered in the experiments, one was a sessile droplet heated by a hotplate and the other was a droplet heated by an electrode at the apex. Micro-PIV system was also used in the experiments to obtain the flow rate inside the droplet. Both experiments showed good accordance with the theoretical explanation of Marangoni convection.

2. Theory

In the interior of a liquid, a molecule is in contact with 4–12 other molecules [1]. However, at the interface between liquid and gas, because of the low density of gases, this number is much smaller (mathematically half of the bulk molecules) [1]. At the macroscopic scale, the physical quantity named ‘surface tension’ is introduced to describe this molecular effect. The value of the surface tension depends on the temperature in the Guggenheim–Katayama formula [1] as:

$$\gamma = \gamma^* \left(1 - \frac{T}{T_c}\right)^n, \tag{1}$$

where γ^* is the surface tension when the temperature is T_c. T_c is the critical temperature in Kelvin and n is an empirical parameter. Considering that n is close to 1

and using a measured reference value γ_0 ($T = 0°C$), this formula becomes a linear approximation [1]:

$$\gamma = \gamma_0(1 + kT), \tag{2}$$

where k is the temperature coefficient of surface tension, for water it is $-0.0015°C$. Because of this, if the temperature varies from one region to another on a sessile droplet, the surface tension will be non-uniform on the surface, thus, liquid will flow from the region with lower surface tension to where surface tension is higher. This kind of fluid flow represents thermal Marangoni convection.

Marangoni convection occurs if the variation in the surface tension force dominates the viscous force. The Marangoni number *Ma*, a dimensionless number, determines the strength of the convection motion

$$Ma = \frac{\Delta\gamma R}{\rho\nu\alpha}, \tag{3}$$

where R is the radius of the spherical cap, ρ the density of the liquid, ν the kinematic viscosity, α the thermal diffusivity and $\Delta\gamma$ the surface tension difference between the cooler region and the warmer region of the surface. *Ma* number represents the ratio between the surface tension force and the viscous force [21].

3. Experimental Setup

3.1. Thermal Imaging System

In order to observe the thermal Marangoni convection on the surface of the droplets, an IR thermal imager was used in the experiments. The IR thermal imager used was Fluke Ti-55. Since the dimension of the droplets was as small as 1 mm, a close-up lens especially designed for the thermal imager was also included. The resolution of the thermal imager is 320 × 240 at 60 fps frame rate and the accuracy is 0.05°C (shown as Fig. 1).

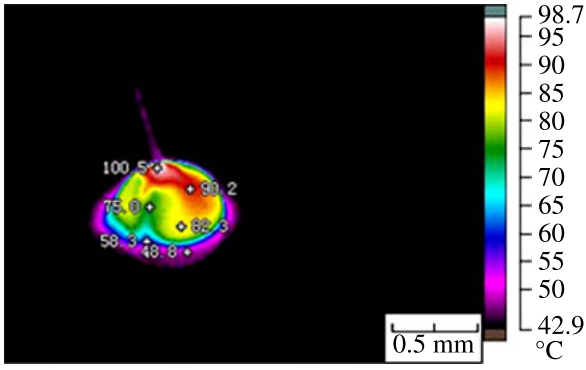

Figure 1. Thermal image of a heated droplet.

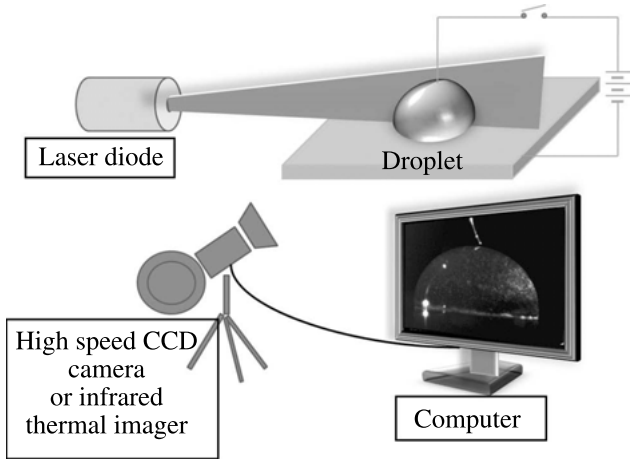

Figure 2. Schematic of micro-PIV system (top) and thermal imaging system (bottom).

3.2. Micro-PIV System

Though the thermal imager is capable of observing the temperature distribution in the droplet *in situ*, it can only measure the temperature on the surface of the droplet. As a consequence, micro-PIV system was also used to visualize the inner fluid field in the droplets.

Shown in Fig. 2, the micro-PIV system consisted of a high power red laser diode (100 mW, $\lambda = 365$ nm), a precisely adjusted lifting platform, a regulated DC voltage source (maximum voltage 1000 V) and a high frequency microscopic charge-coupled device (CCD) camera (1000 frames per second). A solution of 0.1 mol/l KCl and glass balls of 10 μm diameter as particles were used in the experiment. Red laser coming from the diode would brighten the particles suspended in the droplet and with the help of the CCD camera, the inner fluid field was pictured directly. Particles used in the experiments were supplied by the Beijing Lifangtiandi Sci&Tech Ltd. Co., whose diameter was 10 μm and density was 1.3 g/cm^3 [21]. The laser beam passed an adjustable narrow gap and then passed across the middle of the droplet, so that only the fluid field in this section of the droplet was recorded. The fluid field video recorded by the camera was further processed by professional PIV software FlowManager 4.7 to obtain the flow velocity [18, 22, 23].

4. Experimental Results and Discussion

4.1. Sessile Droplet on a Hotplate

As explained, the fluid field inside the droplet which is heated by a hotplate is supposed to be as shown in Fig. 3. As the droplet is heated by a hotplate, the bottom of the droplet reaches a higher temperature than the other parts of the droplet. With the occurrence of the temperature gradient, the surface tension of droplet becomes uneven between the bottom and the apex. The warmer region at the bottom has

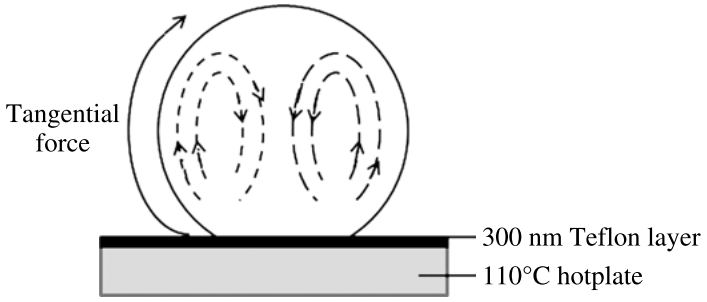

Figure 3. Schematic of thermal Marangoni convection. Non-uniformity of surface tension caused by temperature gradient on the surface of droplet results in two vortices in the cross section of the droplet.

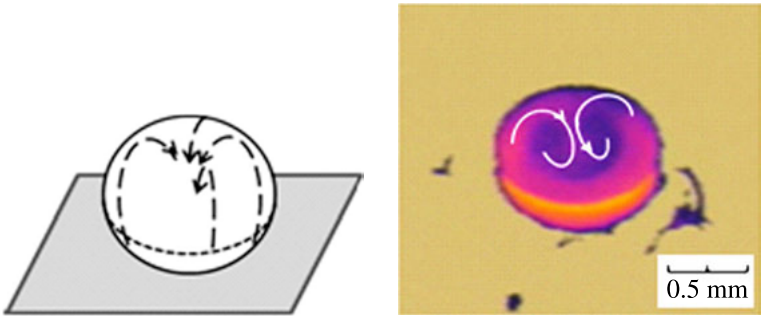

Figure 4. Thermal Marangoni convection in the sessile droplet on the hot surface. (a) Schematic of the surface flow. (b) Thermal image of the heated droplet. Blue heart-like vortex at the apex shows the flow velocity on the surface.

lower surface tension than the cooler region at the apex, consequently, liquid flows upwardly on the surface and downwardly inside the drop. So the convection in the droplets heated by a hotplate should be upward at the surface and downward in the bulk.

In the experiments, the convection flow could be observed clearly with IR thermal imaging (Fig. 4). In the picture, color more close to red represents high temperature and blue refers to low temperature. The *Ma* number is about 7.01×10^4 from equation (3), where the radius of droplet is 1 mm and the temperature difference reaches 30°C, other parameters used in the calculation are shown in Table 1. Since the particles used in the experiment might change the surface tension of liquid, the surface tension of sample solution with particles was measured and shown in Table 2. From the video taken by the thermal imager, warmer liquid surface, region in orange in Fig. 4(b), close to the substrate flowed upwardly to the apex, the blue heart-like area, and a vortex appeared at the apex. The hotplate was heated up to 110°C in order that the bottom of the droplet would maintain a higher temperature than the other parts of the droplet surface. Though the temperature was over 100°C, the droplet could stay still for a few seconds on the hot surface before being

Table 1.
Parameters used in the calculation of Marangoni number [26, 27]

Radius of droplet R (mm)	1
Density of water ρ (kg·m^3)	10^3
Thermal diffusivity α (m^2/s)	0.14×10^{-6}
Kinematic viscosity ν (m^2/s)	8.94×10^{-7}

Table 2.
Surface tension at different temperatures of sample liquid (0.1 mol/l KCl solution with glass particles)

Temperature T (°C)	Surface tension γ (mN/m)
68.0	56.0
77.7	53.6
90.4	50.8
96.9	47.2

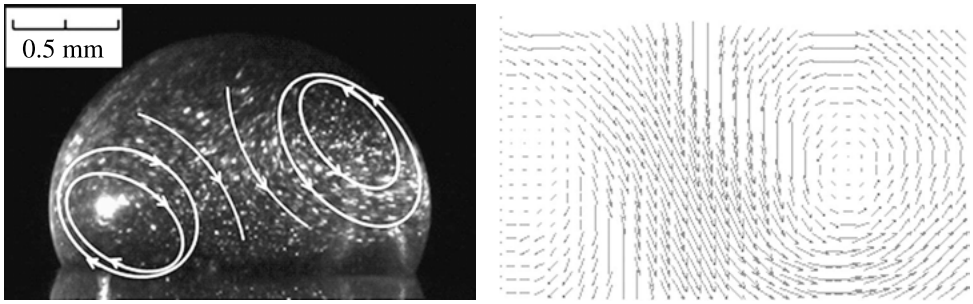

(a) (b)

Figure 5. PIV images of the bulk liquid in the droplet. (a) Two vortices due to Marangoni convection are shown. (b) Visualized flow field of (a), showing the flow velocity.

totally evaporated. From the video file, the hot surface liquid flowed rapidly from the substrate to the apex, and though the fluid velocity could not be measured, the fluid field was qualitatively in accord with the theoretical analysis of Marangoni convection.

To supplement the thermal image, a micro-PIV experiment was carried out to ascertain the exact flow velocity in the droplets. Figure 5 shows the PIV image taken by the microscopic CCD camera. The vortex in the interior of the droplet is seen clearly in the photograph. From the visualized flow field (Fig. 5(b)), the flow velocity was quantified. At the very center of the droplets, the flow rate reaches the maximum, about 23 mm/s. In the center of the vortex, the particles in the picture

almost stay still and the velocity is down to zero. The two vortices are not perfectly symmetrical and this might be caused by non-uniform temperature of the hotplate.

4.2. Sessile Droplet Heated by an Electrode at the Apex

In the experiment on a sessile droplet heated by an electrode, a droplet of KCl solution was trapped between PDMS hydrophobic layer and indium tin oxide (ITO) glass hydrophilic area (Fig. 6). A platinum electrode with a diameter of 100 μm touched the apex of the droplet, consequently, current passed through the droplet between the electrode and the ITO conductive glass. The droplet was heated by the electric current. Theoretically, the heated surface region should develop as the dashed line profile in Fig. 6 because of the same reason as in the case of hotplate heating situation. Since the cross section is small at the apex, the current density is high and Joule heat is generated there (Fig. 7). In the picture, the maximum surface

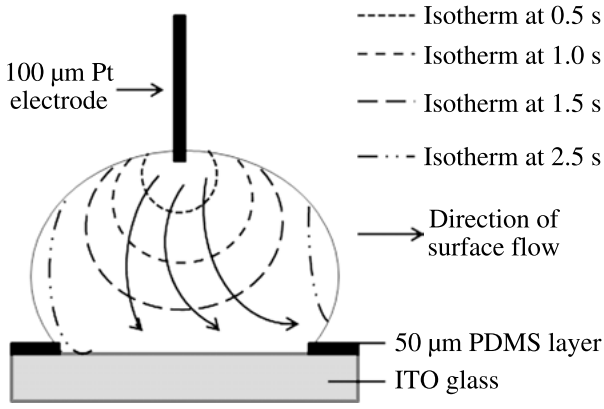

Figure 6. Schematic of surface flow in the droplet heated by an electrode on the apex. The isotherms at different times are indicated in the picture to show the development of the temperature field at the surface.

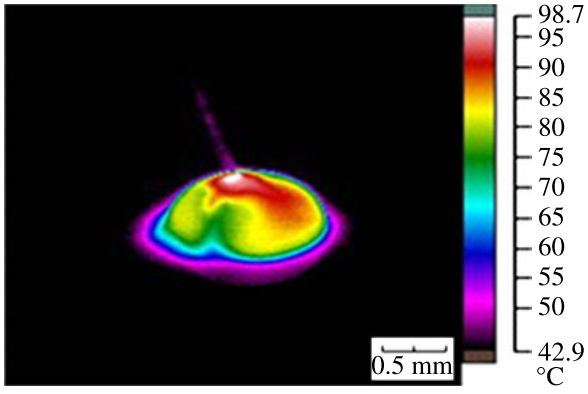

Figure 7. Temperature distribution on the droplet surface when the electrode contacts the droplet. Red color refers to a higher temperature while blue refers to a cooler region.

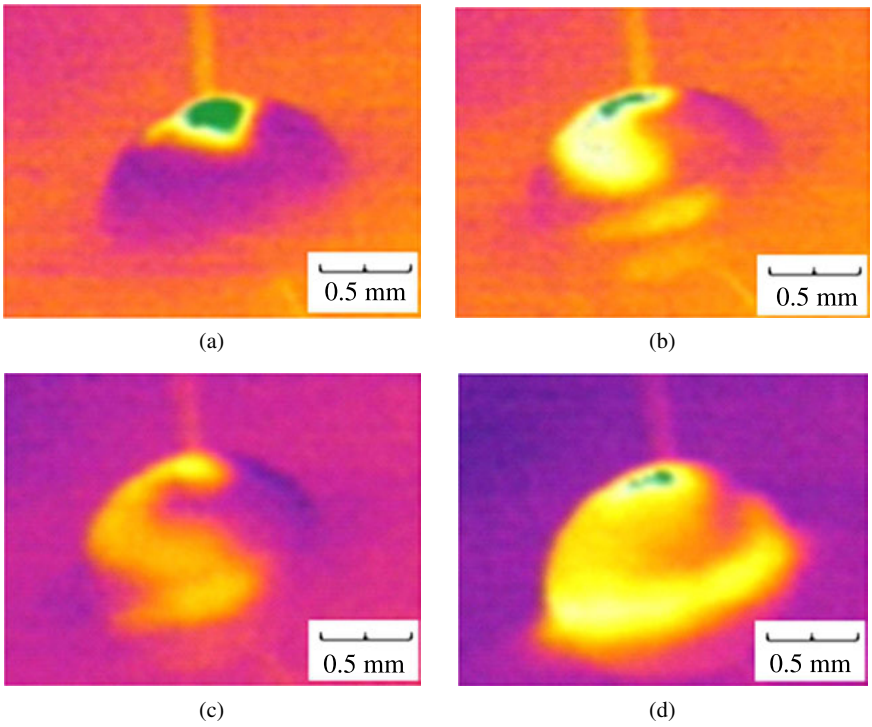

Figure 8. Evolution process of temperature distribution. Pictures are taken in series every 0.5 s.

temperature is achieved in the region with red color (reaches nearly 100°C), and it flows downwards to the bottom of the droplet (60 V DC voltage applied). In this case, the *Ma* number of the droplet is 4.24×10^4 from (equation (3)), where $R = 1$ mm and $\Delta T = 20$°C (Tables 1 and 2). The process is recorded in Fig. 8. At the beginning of the process, liquid surface close to the electrode reaches a higher temperature. Because of the existing temperature gradient between the apex and the bottom, the liquid at the apex is pulled down to replace the cooler liquid at the bottom. The four thermal images were taken in series with a constant time interval of 0.5 s, and these agreed well with the theory of Marangoni convection.

In micro-PIV image, the interior flow field is clearly seen (Fig. 9). Two symmetrical vortices appear immediately on touching of the electrode and the droplet. In the center of the droplet, the particles in the solution move swiftly from the floor electrode (ITO conductive glass) to the roof electrode (Pt electrode). The flow velocity in the center reaches the maximum, about 17.5 mm/s. In the center of the vortex, the particles stay still and the velocity drops to zero.

5. Discussion

Though the temperature of the liquid in both experiments was as high as 100°C; the variation of temperature in the droplet was no higher than 30°C, as a consequence,

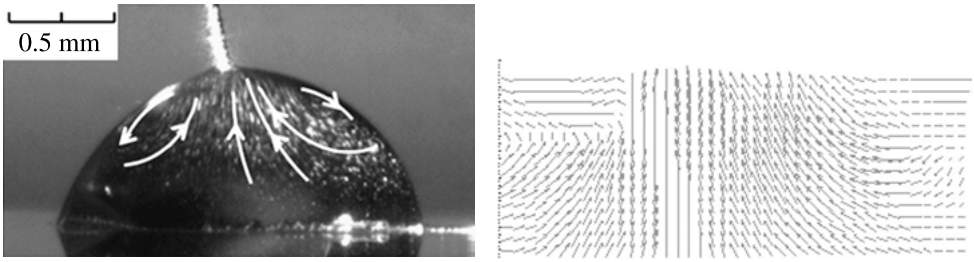

Figure 9. PIV images of the droplet heated by an electrode. (a) Vortices formed with an upward stream in the center. (b) Visualized flow field processed by the computer.

the variation of density of water would be as small as 1% (the density of water is 958.4 kg/m^3 at 100°C, 971.8 kg/m^3 at 80°C). Because of the small variation in density, the gravity-driven flow was negligible. On the other hand, the duration of the observation was short (smaller than 3 s in both experiments), so the influence of evaporation of liquid could be ignored.

These *Ma* numbers are of the same order as in Chai and Arpaci's work [24], where the *Ma* number reached as high as 10^4 for a water droplet with a radius of 1 mm, evaporating in a relatively mild environment. Since the critical value of the Marangoni number $Ma_c = 80$ [21, 24, 25] which is several orders smaller than the *Ma* number in this paper, the surface tension force dominates the viscous force. The viscous force then creates momentum in the droplet and a Marangoni flow is formed [21]. Compared with the former experiment, the temperature variation in the droplet heated by an electrode is as small as 20°C. Consequently, the *Ma* number of this droplet is relatively smaller than that of droplet heated by a hotplate. Since the *Ma* number determines the strength of the convection motion, the flow velocity in the latter experiment was smaller than in the former case. Though the surface tension of sample liquid (Table 2) is different from pure water (58.9 mN/m at 100°C), the difference is no more than 20%, which means that the presence of solute and particles does not influence the convection mode of the liquid (the change in *Ma* number is less than 20%). Furthermore, the related experimental research on evaporation of sessile droplet is systematically carried out [28].

6. Conclusions

An *in situ* observation method for thermal Marangoni convection in a sessile droplet using IR thermal imaging was introduced. Two types of thermal Marangoni convections were observed in the experiments: (1) a sessile droplet heated by a hotplate; (2) a sessile droplet heated by an electrode at the apex. In the droplet heated by a hotplate, thermal image clearly showed that the surface liquid flows upwards to the apex due to the temperature gradient between the bottom and the apex of the droplet which agreed well with the theoretical prediction and the work of other researchers.

In addition, a micro-PIV system was applied to validate the bulk flow field in the droplet. Thermal image of the droplet showed that surface liquid which was first heated by the electrode flows downwards towards the substrate, and the micro-PIV image substantiated the results.

Acknowledgements

This work was jointly supported by National Natural Science Foundation of China (NSFC, Grant Nos 11072244 and 60936001) and Instrument Developing Project of the Chinese Academy of Sciences (Grant No. Y2010031). The authors are grateful to Prof. Li Duan and Dr Lujun Li from the National Microgravity Laboratory, Institute of Mechanics, Chinese Academy of Sciences, for fruitful discussions. The authors are also thankful to Mr Xiaozhuo Zhai from the Fluke Corporation for the invaluable support in the use of various equipments.

References

1. J. Berthier, *Microdrops and Digital Microfluidics*. William Andrew, Norwich, NY (2008).
2. Q. Z. Yuan and Y. P. Zhao, *Phys. Rev. Lett.* **104**, 246101 (2010).
3. Y. Huo and B. Li, *Int. J. Heat Mass Transf.* **47**, 3533 (2004).
4. F. Schönfeld, K. H. Graf, S. Hardt and H. J. Butt, *Int. J. Heat Mass Transf.* **51**, 3696 (2008).
5. G. Li, K. Graf, E. Bonaccurso, D. S. Golovko, A. Best and H. J. Butt, *Macromol. Chem. Phys.* **208**, 2134 (2007).
6. B. Arendt and R. Eggers, *Int. J. Heat Mass Transf.* **50**, 2805 (2007).
7. V. M. Ha and C. L. Lai, *Int. J. Heat Mass Transf.* **47**, 3811 (2004).
8. Y. Hong, W. Q. Jin, X. H. Pan and Y. Shinichi, *Int. J. Heat Mass Transf.* **49**, 4254 (2006).
9. E. A. Guggenheim, *J. Chem. Phys.* **13**, 253 (1945).
10. W. C. Jia and H. H. Qiu, *Int. J. Heat Mass Transf.* **45**, 4141 (2002).
11. W. Dai and Y. P. Zhao, *J. Adhesion Sci. Technol.* **22**, 217 (2008).
12. J. M. Andrew, *Lab Chip* **1**, 24N (2001).
13. R. H. Farahi, A. Passian, S. Zahrai, A. L. Lereu, T. L. Ferrell and T. Thundat, *Ultramicroscopy* **106**, 815 (2006).
14. A. Passian, S. Zahrai, A. L. Lereu, R. H. Farahi, T. L. Ferrell and T. Thundat, *Phys. Rev. E* **73**, 066311 (2006).
15. R. H. Farahi, A. Passian, T. L. Ferrell and T. Thundat, *Opt. Lett.* **30**, 616 (2005).
16. R. H. Farahi, A. Passian, L. Ferrell and T. Thundat, *Appl. Phys. Lett.* **85**, 4237 (2004).
17. J. T. Feng and Y. P. Zhao, *J. Phys. D: Appl. Phys.* **41**, 052004 (2008).
18. S. H. Ko, H. Lee and K. H. Kang, *Langmuir* **24**, 1094 (2008).
19. J. Wu, W. B. Cao, W. J. Wen, D. C. Chang and P. Sheng, *Biomicrofluidics* **3**, 012005 (2009).
20. L. Y. Lu, S. L. Peng, X. Z. Niu and W. J. Wen, *Appl. Phys. Lett.* **89**, 223521 (2006).
21. J. J. Hegseth, N. Rashidnia and A. Chai, *Phys. Rev. E* **54**, 1640 (1996).
22. L. Duan, Q. Kang and W. R. Hu, *Chin. Phys. Lett.* **25**, 1347 (2008).
23. H. W. Lu, F. Bottausci, J. D. Fowler, A. L. Bertozzi, C. Meinhart and C. J. Kim, *Lab Chip* **8**, 456 (2008).
24. A. T. Chai and V. S. Arpaci, in: *Proceedings of Second Microgravity Fluid Physics Conference*, Cleveland, OH, pp. 141–147 (1994).

25. J. R. A. Pearson, *J. Fluid Mech.* **4**, 489–500 (1958).
26. J. P. Holman, *Heat Transfer*, 9th edn. McGraw-Hill, London (2002).
27. D. R. Lide (Ed.), *CRC Handbook of Chemistry and Physics*, 89th edn. CRC Press, Boca Raton, FL (2008–2009).
28. Y. S. Yu, Z. Q. Wang and Y. P. Zhao, *J. Colloid Interface Sci.* **365**, 254 (2012).